JOURNAL OF GEOPHYSICAL RESEARCH, VOL. 111, D13101, doi:10.1029/2005JD006142, 2006

Relationships between rainfall anomalies over northeastern Brazil and the El Niño–Southern Oscillation

Mary T. Kayano[1] and Rita V. Andreoli[1]

Received 28 April 2005; revised 6 October 2005; accepted 29 March 2006; published 1 July 2006.

[1] In this paper, sea surface temperature (SST) and sea level pressure variability modes associated with climate extremes (droughts and floods) over northeastern Brazil (NEB) stratified according to the El Niño–Southern Oscillation (ENSO) phases (El Niño, La Niña, and neutral) are reexamined. The analyses indicate that only 36% of the time an ENSO-based forecast for the NEB climate would be right. This relatively low percentage is mostly because the interannual variations of the NEB climate are more closely tied to the tropical South Atlantic SST variability modes than to the tropical Pacific variability mode. An interesting aspect revealed in the present analysis is that hints of the February–April SST anomaly patterns in the tropical Atlantic for dry and wet cases which are not directly related to the ENSO can be found months prior to the NEB rainy season. Since these hints are particularly strong in the tropical South Atlantic, the SST variations in this sector during months prior to the rainy season should be carefully monitored in the diagnostic activities.

Citation: Kayano, M. T., and R. V. Andreoli (2006), Relationships between rainfall anomalies over northeastern Brazil and the El Niño–Southern Oscillation, *J. Geophys. Res.*, *111*, D13101, doi:10.1029/2005JD006142.

1. Introduction

[2] The interannual climate variability over northeast Brazil (NEB), with the occurrence of extreme droughts and also floods in some years, is the main factor that impacts the social and economic life of the local population. Part of this variability is explained by El Niño–Southern Oscillation (ENSO) related large-scale climate teleconnections, which were diagnostically evidenced in several studies [*Walker*, 1927; *Caviedes*, 1973; *Hastenrath and Heller*, 1977; *Kousky et al.*, 1984; *Ropelewski and Halpert*, 1987, 1989; *Aceituno*, 1988; *Kayano et al.*, 1988; *Kiladis and Diaz*, 1989; *Rao and Hada*, 1990].

[3] A reduction in the NEB precipitation observed during some warm ENSO (or El Niño (EN)) episodes has been attributed to large-scale changes in an eastward displaced Walker circulation with its rising branch over eastern equatorial Pacific, where abnormally warm surface waters prevail, and its sinking branch over tropical Atlantic [*Kousky et al.*, 1984; *Kayano et al.*, 1988]. On the other hand, the increased precipitation in this same region noted during some cold ENSO (or La Niña (LN)) episodes is explained by nearly reversed anomalous patterns of atmospheric circulation and sea surface temperature (SST) [*Kousky and Ropelewski*, 1989]. Concerning the northern and northeastern sectors of South America, *Ropelewski and Halpert* [1987, 1989] found dry conditions in the areas which comprise Venezuela, Guyana, Surinam, French Guiana and the equatorial areas of Brazil during July$^{(0)}$–March$^{(+)}$ for EN episodes, and wet conditions in this area during June$^{(0)}$–March$^{(+)}$ for LN episodes. The superscripts "(0)" and "(+)" indicate the onset year of an ENSO extreme and the following year, respectively.

[4] *Aceituno* [1988], studying the annual cycle of correlation patterns between the Southern Oscillation index (SOI) and the rainfall series for several South American stations, found significant correlations mainly in the northern portion of the NEB during March–April. However, correlations of 0.4 or less between the SOI and the rainfall anomaly series in the NEB found in previous studies [*Aceituno*, 1988; *Rao and Hada*, 1990] are considered relatively low [*Kane*, 1992, 1997]. In addition, only 46% of the EN episodes of the 1849–1992 period were associated with droughts in the northern sector of the NEB [*Kane*, 1997]. So, a significant part of the total interannual rainfall variability in the NEB might not be explained by ENSO extremes.

[5] Other factors, besides the ENSO, which take relevant part in the interannual climate variability over NEB are associated with the tropical Atlantic SST variability. Indeed, severe droughts in the NEB have been associated with the presence of negative SST anomalies in the tropical south Atlantic [*Markham and McLain*, 1977]. Moreover, a SST variability mode in the tropical Atlantic displaying an asymmetric SST anomaly pattern about the equator has long been related to interannual climate variations over NEB [e.g., *Weare*, 1977; *Hastenrath and Heller*, 1977; *Hastenrath*, 1978; *Moura and Shukla*, 1981; *Hastenrath*, 1990; *Hastenrath and Greischar*, 1993; *Nobre and Shukla*, 1996; *Souza et al.*, 2000]. This mode has been referred to as a SST dipole mode [*Servain*, 1991].

[6] The dynamics involved in this mode is in such a way that the cross-equatorial SST gradient pattern induces an anomalous thermally direct meridional circulation which

[1]Instituto Nacional de Pesquisas Espaciais, Centro de Previsão de Tempo e Estudos Climáticos, São José dos Campos, Brazil.

0148-0227/06/2005JD006142$09.00

affects the position and intensity of the Intertropical Convergence Zone (ITCZ), which in turn modulates the NEB rainfall [*Moura and Shukla*, 1981]. A similar interpretation is that droughts in the NEB are associated with an oceanic-atmospheric pattern featuring an anomalously northward displaced ITCZ, reduced northeast trade winds, accelerated cross-equatorial northward flow, positive SST anomalies in the tropical North Atlantic, and negative SST anomalies in the tropical South Atlantic [*Hastenrath*, 1990; *Hastenrath and Greischar*, 1993]. *Pezzi and Cavalcanti* [2001], using modeling results, showed that the dipole mode plays more a crucial role in the NEB rainfall interannual variations than the ENSO mode.

[7] Nevertheless, some authors suggest that SST fluctuations in the two sides of the tropical Atlantic are not related to each other from interannual to decadal time scales due to the fact that the SST anomaly time series for the northern and southern sides of this basin are not correlated [*Mehta*, 1998; *Rajagopalan et al.*, 1998; *Enfield et al.*, 1999]. Furthermore, the SST dipole mode is dominated by decadal variations [e.g., *Mehta and Delworth*, 1995; *Tourre et al.*, 1999; *Andreoli and Kayano*, 2003]. In addition, the two sides of the tropical Atlantic seem to have unbalanced influences on the NEB rainfall variations. *Moura and Shukla* [1981] correlating the normalized rainfall anomalies averaged for Fortaleza and Quixeramobim with the tropical Atlantic SST anomalies found positive correlations of up to 0.7 in the southern side contrasting with negative correlations of up to −0.4 in the northern side (their Figure 3). In this context, *Kane* [1992], using the SST indices defined by *Servain* [1991], provided evidences that Fortaleza rainfall variations have stronger relations to the southern than to the northern sector of the tropical Atlantic.

[8] So both the tropical Pacific and Atlantic Oceans play important roles in the interannual climate variability over NEB. While the tropical Pacific operates through a single interannual ENSO mode, the tropical Atlantic might operate through at least five interannual SST modes (two separate modes in both sides of the basin, equatorial mode, dipole-like mode and cross-equatorial SST gradient mode). *Andreoli and Kayano* [2003] showed that the Atlantic SST modes are evolving modes in a decadal time scale evolution.

[9] Previous studies on the NEB climate classified the years according to the climate extremes (dry or wet) and identified the corresponding SST Atlantic modes [*Hastenrath and Heller*, 1977; *Hastenrath and Greischar*, 1993]. Others identified the ENSO extremes and obtained the related precipitation anomaly patterns over NEB [*Ropelewski and Halpert*, 1987, 1989; *Kayano et al.*, 1988]. *Barros and Silvestri* [2002] analyzed the differences in the rainfall variability over southern South America among EN (LN) events. Here a similar approach is used by stratifying the NEB climate extremes (as reflected in the precipitation) according to the ENSO phases (EN, LN, and ENSO neutral).

[10] So, the present work will use 87 years of monthly data to revise the relationship between seasonal (from February to April (FMA)) rainfall anomalies over NEB and the ENSO as reflected in the SST and SLP anomalous patterns. Data and methodology are described in section 2, relations of the NEB seasonal rainfall and the large scale anomaly composites are described in section 3. Because the tropical Atlantic variability plays an important role in the NEB climate, bimonthly SST anomaly patterns in this sector for periods prior to the NEB rainy season are also analyzed in section 3. Conclusions are given in section 4.

2. Data and Methodology

[11] The data sets used in this paper consist of reconstructed monthly SST series for the 1854–2000 period obtained by *Smith and Reynolds* [2003] and monthly SLP data for the 1871–1994 period obtained from the British Atmospheric Data Centre Web site (http://www.badc.rl.ac.uk/). The SST and the SLP data are at 2° by 2° and at 5° by 5° latitude-longitude resolution grids, respectively. Analyses of the SST data are done for the area bounded at 45°N, 45°S, 120°E and 30°E. On the other hand, analyses of the SLP data are limited on the global band between 80°N and 60°S.

[12] Forty four gridded monthly precipitation series in the South American area bounded at 10°N, 15°S, 70°W and 35°W for the 1912–1998 period are extracted from "gu23wld0098.dat" (version 1.0) constructed and provided by Mike Hulme. This data set is described by *Hulme* [1992, 1994] and by *Hulme et al.* [1998]. Locations of 44 grid points used in the present study are illustrated in Figure 1. The area covered by these grid points includes not only the NEB but also most of the Amazon region.

[13] Monthly anomalies of SST and SLP and precipitation at each grid point are obtained as departures from the 1912–1998 means. These anomaly series at each grid point are normalized by the corresponding standard deviation of the anomaly time series. The normalized SST anomalies at each grid point are linearly detrended.

[14] Because of the data resolution, the Niño-3 SST index is calculated here as the 5-month running mean of the averaged SST anomalies in the area bounded at 4°N, 4°S, 150°W and 90°W. This index is then, linearly detrended. Using the criterion suggested by *Trenberth* [1997], an EN (a LN) event is identified when the detrended Niño-3 SST index exceeds (is less than) the threshold of 0.5°C (−0.5°C) for at least six consecutive months.

[15] A rainfall index is defined considering that the ENSO and tropical Atlantic variability affect most of the NEB [*Ropelewski and Halpert*, 1987, 1989; *Souza et al.*, 2000]. So, the FMA season is analyzed because it encompasses the three rainiest months in the central and western NEB [*Rao and Hada*, 1990]. Twelve grid points with their rainy seasons overlapping at least two months of the FMA season and their dry seasons overlapping at least 2 months of the period from August to October are selected (large dots in Figure 1). The oceanic grid points off the NEB coast are due to the interpolation used by *Hulme* [1992, 1994]. First, area averaged rainfall values are obtained from the rainfall data of the selected grid points. A seasonal series is then calculated by totalizing the area averaged monthly values from February to April.

[16] The analyses focus on the relationships between the seasonal (FMA) rainfall over NEB and the ENSO phases in the preceding year. So, the seasonal rainfall values for the period from 1913 to 1998 are ranked from 1 for the smallest value to 86 for the largest value. The ranked amounts are

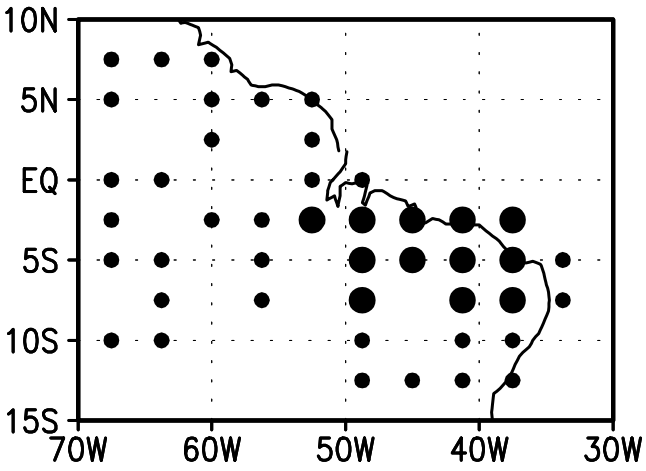

Figure 1. Locations of the 44 rainfall grid points. Large dots indicate the grid points used to calculate the NEB rainfall index for FMA.

divided by 86. The resulting percentile ranks (R) varying from approximately zero to 1 are then used to classify the NEB climate.

[17] For a given ranked precipitation series (with one value per year), years with $0.33 < R < 0.66$ are normal years, while those with $R \leq 0.33$ and $R \geq 0.66$ are dry years and wet years, respectively [*Pinkayan*, 1966]. Using this criterion, the seasonal ranked series are classified in dry, normal and wet categories, which are stratified according to the ENSO phases (EN, LN and neutral) of the preceding year. Table 1 lists the onset years of ENSO phases followed by dry, wet or normal conditions in the NEB during FMA. The EN, LN and ENSO neutral years followed by a dry rainy season in the NEB (dry cases) are referred to as DRY-EN, DRY-LN and DRY-NE, respectively. Similarly, the LN, EN, and ENSO neutral years followed by a wet rainy season in the NEB (wet cases) are referred to as WET-LN, WET-EN, and WET-NE, respectively. The cases with normal rainy season in the NEB listed in Table 1 are not analyzed in detail. Interpretation of Table 1 is given in the next section.

[18] Seasonal composites of precipitation, SST, and SLP anomalies for the dry and wet cases are done for the FMA period. Bimonthly composites of SST anomalies in the tropical Atlantic are done for months preceding the rainy season. In order to assess the statistical significance of the composites, the number of degrees of freedom is the number of years. It is assumed that a variable X with n values and S standard deviation shows a Student's t distribution. So, only composites with absolute values exceeding $t_{\alpha(n-1)}S/\sqrt{(n-1)}$ are statistically significant [*Panofsky and Brier*, 1968]. The confidence level of 95% is used.

3. Results

3.1. Classification of the NEB Rainy Season According to the ENSO Phases

[19] Of the 29 drier than normal rainy seasons in the first row of Table 1, 10 were preceded by EN, 8 by LN, and 11 by ENSO neutral years. Of the 30 wetter than normal rainy seasons in Table 1, 6 were preceded by EN, 9 by LN and 15 by ENSO neutral years. Finally, of the 27 normal rainy seasons in Table 1, 8 were preceded by EN, 7 by LN, and 12 by ENSO neutral years. So, of the 59 years with climate extremes in the NEB (first and second rows in Table 1), 19 are explained by the known relationship between the NEB rainfall anomalies and the ENSO. Since these 19 years account for 32% of the total years with climate extremes, the remaining 68% of these years is not explained by the ENSO teleconnections. These 19 rainy seasons together with the 12 normal rainy seasons preceded by ENSO neutral conditions, account for 36% of the total 86 rainy seasons. So, ENSO-based climate forecast for the NEB would be right only 36% of the times. Therefore other factors responsible for climate extremes are analyzed in the sections 3.2–3.4.

3.2. Seasonal Precipitation Composites

[20] The precipitation anomaly composites for the DRY-EN and WET-LN cases show approximately reversed sign patterns, with significant negative and positive values respectively, extending from the NEB to the eastern central Amazon and with small anomalies in the rest of the study domain during FMA (Figures 2a and 2d). These composites display the largest extension of the significant precipitation anomalies among dry and wet composites. The reversed sign patterns for the DRY-EN and WET-LN cases are more conspicuous in the northern sector of the NEB. So, the precipitation in this area shows approximately linear response to the ENSO. These composites describe the ENSO-related regional rainfall anomaly patterns highly consistent with previous findings [*Ropelewski and Halpert*, 1987, 1989; *Rao and Hada*, 1990; *Uvo et al.*, 1998].

[21] The precipitation anomaly composites for the DRY-LN and DRY-NE cases show quite similar patterns, but

Table 1. Classification of the Northeast Brazil Rainy Season According to the ENSO Phases

	ENSO		
NEB Condition	El Niño	La Niña	Neutral
Dry (29)	(10) 1914, 1918, 1940, 1941, 1953, 1957, 1965, 1979, 1982, 1997	(8) 1917, 1936, 1942, 1950, 1954, 1955, 1967, 1971	(11) 1927, 1929, 1931, 1932, 1935, 1943, 1978, 1981, 1989, 1992, 1996
Wet (30)	(6) 1925, 1951, 1963, 1972, 1987, 1994	(9) 1922, 1933, 1938, 1944, 1973, 1975, 1984, 1985, 1995	(15) 1912, 1919, 1920, 1923, 1934, 1937, 1945, 1946, 1960, 1962, 1966, 1980, 1983, 1990, 1993
Normal (27)	(8) 1913, 1930, 1939, 1968, 1969, 1976, 1986, 1991	(7) 1916, 1924, 1949, 1964, 1970, 1974, 1988	(12) 1915, 1921, 1926, 1928, 1947, 1948, 1952, 1956, 1958, 1959, 1961, 1977

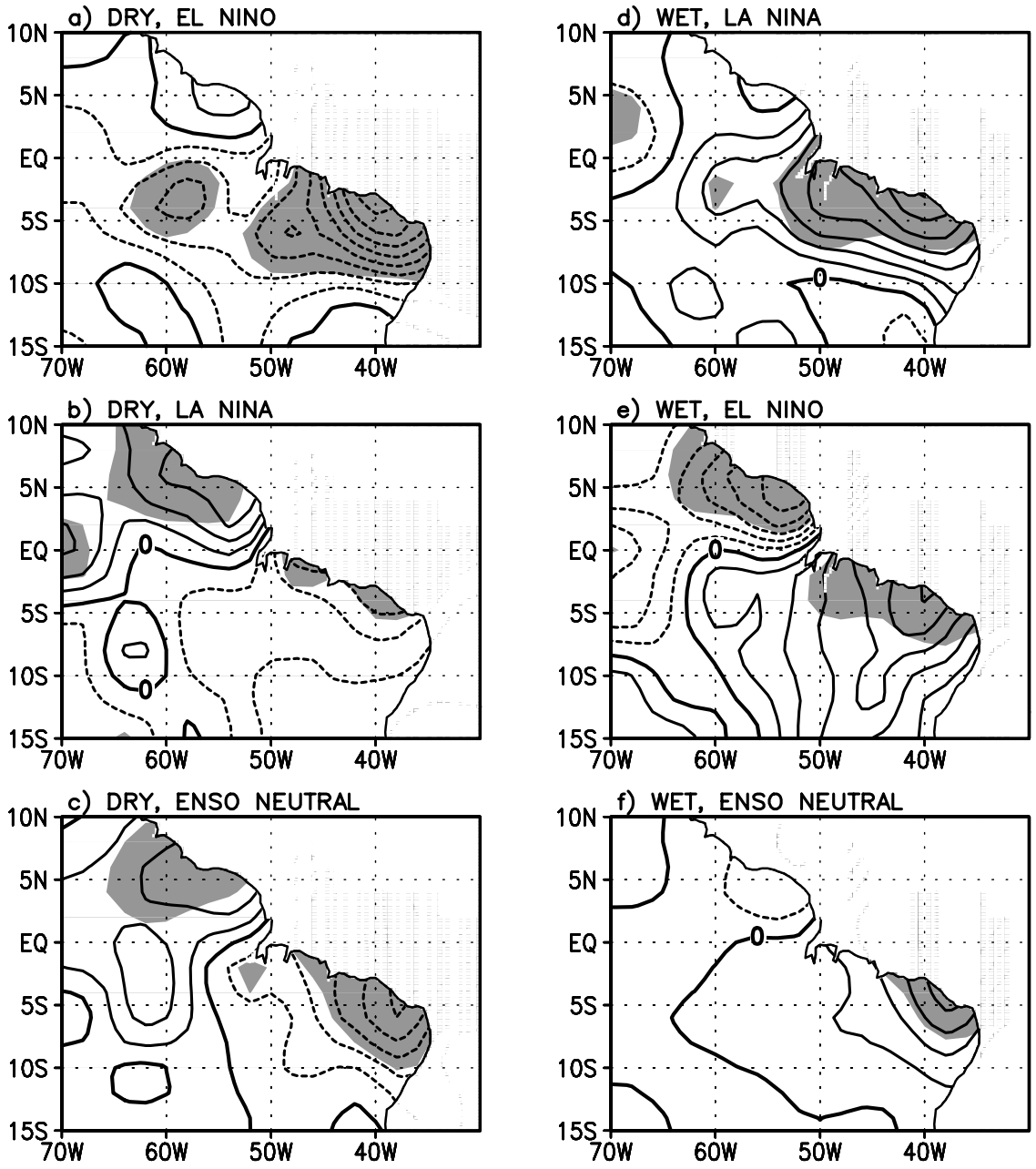

Figure 2. Mean normalized rainfall anomalies during FMA for the cases (a) DRY-El Niño, (b) DRY-La Niña, (c) DRY-ENSO neutral, (d) WET-La Niña, (e) WET-El Niño, and (f) WET-ENSO neutral. Contour interval is 0.2 standard deviations, with negative (positive) contours being dashed (solid). Shading area encompasses values which are significant at the 95% confidence level.

differences in the magnitudes and in the extensions of the significant anomalies. These composites show below normal rainfall in most of the NEB with significant values in its northern sector, and above normal rainfall in the northeastern Venezuela, Guyana, Surinam and French Guiana (Figures 2b and 2c). The precipitation anomaly composites for the WET-EN and WET-NE cases (Figures 2e and 2f) are also similar and show approximately reversed sign patterns of the DRY-LN and DRY-NE cases, respectively. The precipitation composites for the DRY-LN, DRY-NE, WET-EN, and WET-NE cases illustrate the reversed sign precipitation anomalies over NEB and over the region from northeastern Venezuela to French Guiana pointed out in previous studies [*Hastenrath and Heller*, 1977; *Hastenrath*, 1978]. The WET-NE and the DRY-NE cases show small magnitude of the precipitation anomalies over the region from northeastern Venezuela to French Guiana.

[22] The differences among dry composites and among wet composites are certainly related to different combinations of large scale and regional climate modulating factors. While the DRY-EN and WET-LN cases illustrated the known relationships between the ENSO and NEB rainfall anomalies previously discussed in a number of papers [e.g., *Ropelewski and Halpert*, 1987, 1989; *Rao and Hada*, 1990],

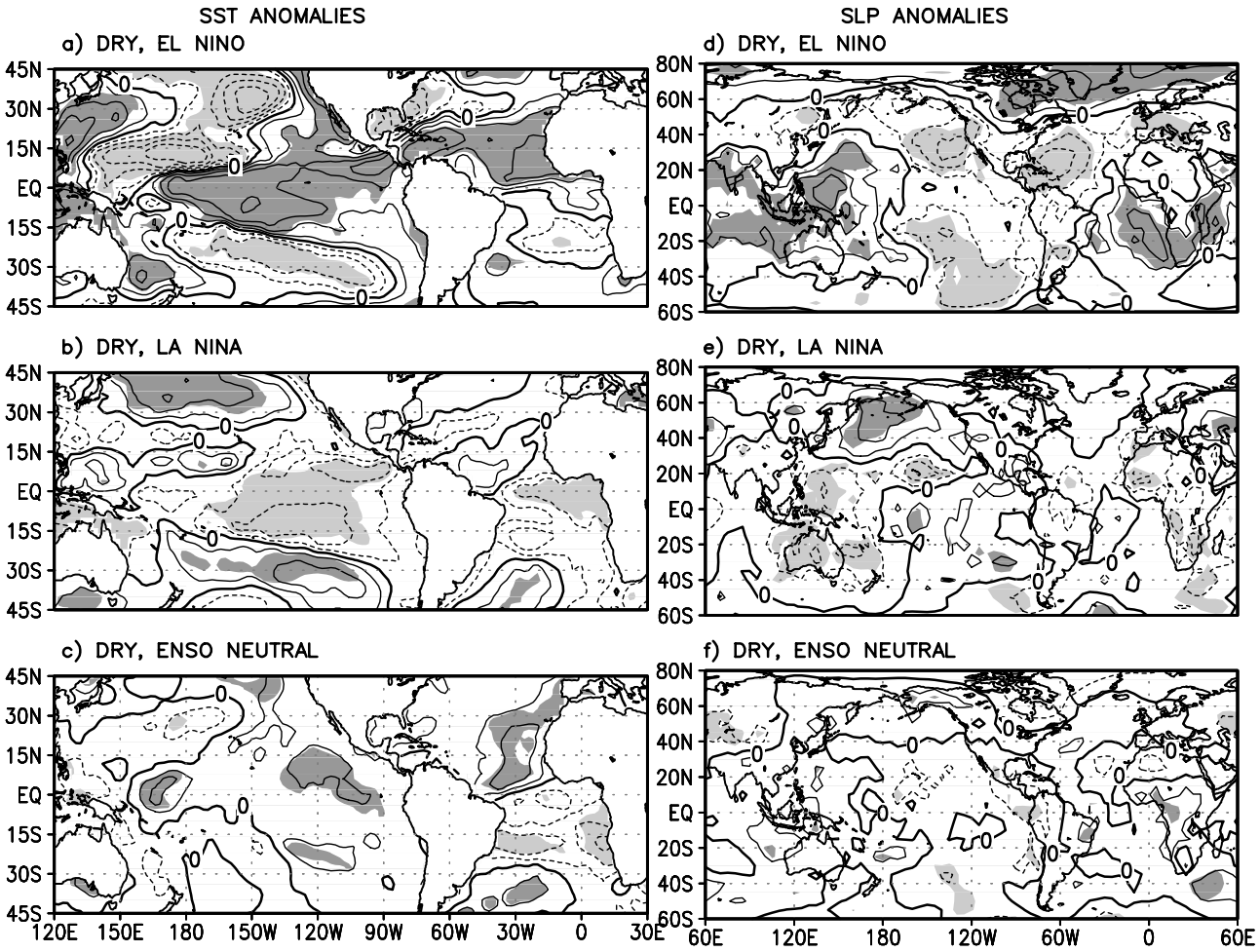

Figure 3. Mean normalized SST anomalies during FMA for (a) DRY-El Niño, (b) DRY-La Niña, and (c) DRY-ENSO neutral. Mean normalized SLP anomalies during FMA for (d) DRY-El Niño, (e) DRY-La Niña, and (f) DRY-ENSO neutral. Contour interval is 0.3 standard deviations, with negative (positive) contours being dashed (solid). Shading encompasses values which are significant at the 95% confidence level.

the other cases might be driven by regional climate monitoring factors. The nearly reversed patterns between DRY-LN and WET-EN cases and between DRY-NE and WET-NE cases suggest that the factors modulating each of these pairs might have the same origin but with opposite effects on the precipitation anomaly patterns. In order to infer the origin of these factors, the dry and wet composites of the SST and SLP anomalies are analyzed in section 3.3 (Figures 3 and 4).

3.3. Large-Scale Seasonal Composites

[23] The SST anomaly pattern for the DRY-EN case presents warmer than normal surface waters in the central and eastern equatorial Pacific flanked to the north and to the south by colder than normal surface waters (Figure 3a). This pattern is similar to that previously described for strong EN [*Rasmusson and Carpenter*, 1982]. This composite also shows significant positive SST anomalies in the tropical North Atlantic, with the largest values close to the coast of Africa and in the Caribbean Sea, and weak anomalies elsewhere in the Atlantic sector (Figure 3a). The SST anomaly pattern in the tropical North Atlantic resembles that of the interannual mode externally forced by the ENSO described in previous work [*Enfield and Mayer*, 1997; *Saravanan and Chang*, 2000]. The associated SLP anomaly pattern features positive values over western tropical Pacific and negative ones to the east, mainly in the southeastern Pacific, two negative centers in the United States region, one in the North Pacific off the west coast and the other in the Gulf coast, and a positive center in the Hudson Bay area (Figure 3d). While the two centers in the eastern side of North America coincide approximately with the locations of the Pacific–North American (PNA) pattern centers in this area, the center in the North Pacific is slightly located to the south of the PNA center and the PNA center near Hawaii is not observed in the present analysis. The PNA pattern was previously associated with interannual teleconnections of a heat source in the eastern tropical Pacific like that due to an EN [*Horel and Wallace*, 1981]. Figure 3d also evidences above normal SLP anomalies centered in the eastern tropical South Atlantic and over NEB. The positive SLP anomalies over NEB and eastern Amazon and the cross-equatorial

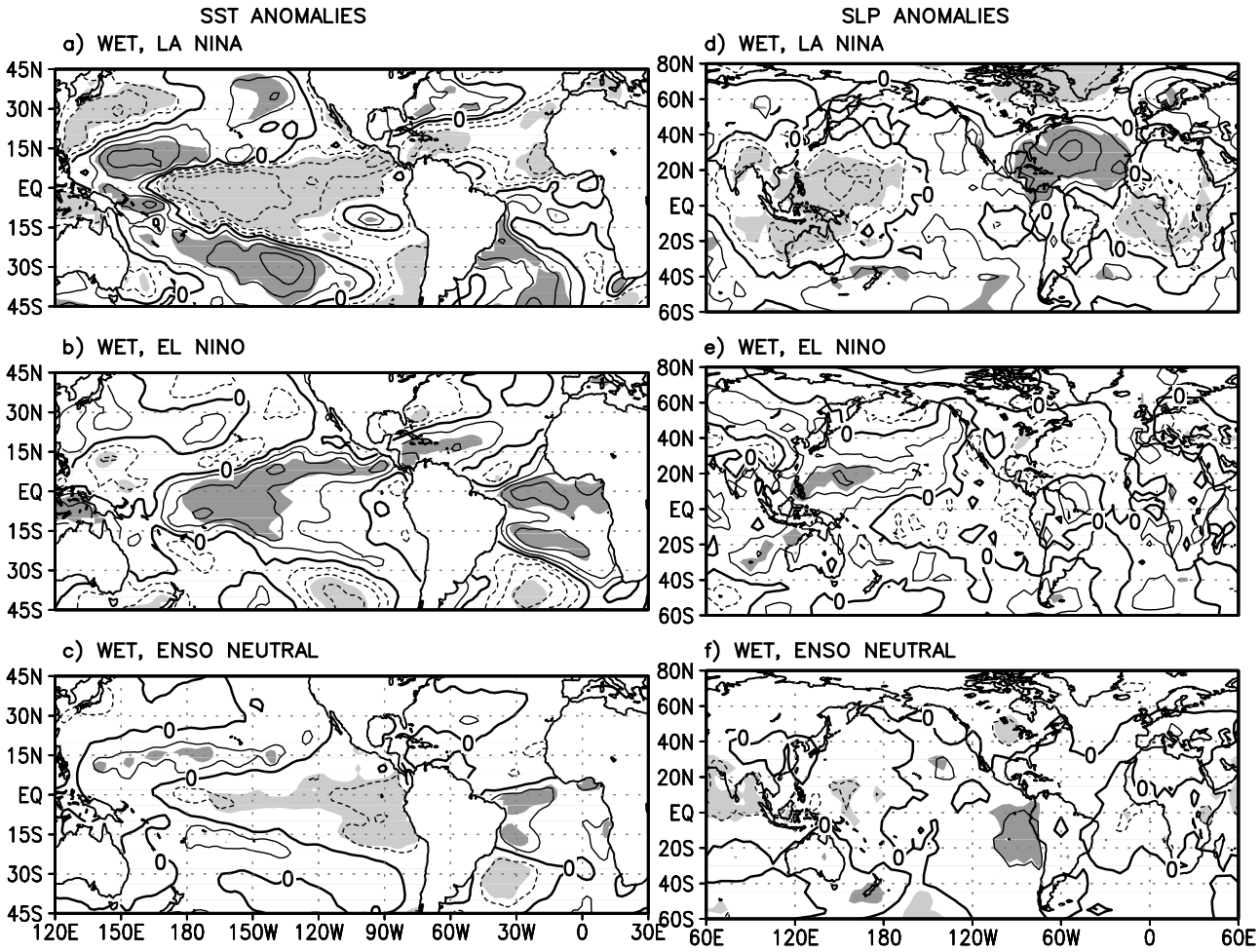

Figure 4. Mean normalized SST anomalies during FMA for (a) WET-La Niña, (b) WET-El Niño, and (c) WET-ENSO neutral. Mean normalized SLP anomalies during FMA for (d) WET-La Niña, (e) WET-El Niño, and (f) WET-ENSO neutral. Display is the same as that in Figure 3.

northward gradient of SST anomalies (positive meridional SST anomaly gradient) in the tropical Atlantic are consistent with the inhibited rainfall over NEB and eastern Amazon. This result confirms previous findings on the role played by the tropical Atlantic SST variability in qualitatively defining the NEB and the eastern Amazon rainy season [*Hastenrath and Heller*, 1977; *Moura and Shukla*, 1981; *Nobre and Shukla*, 1996; *Souza et al.*, 2000].

[24] The SST anomaly pattern for the DRY-LN case resembles that of the LN configuration which features colder than normal surface waters in the eastern central Pacific between 15°N and 20°S and warmer than normal surface waters in the North Pacific between 45°N and 30°N approximately and in the southeastern Pacific (Figure 3b). The interannual mode externally forced by the LN, featuring strong negative SST anomalies in the tropical North Atlantic, is not established. Instead, relatively weak SST anomalies prevail in this sector. On the other hand, colder than normal surface waters along the coast of the African countries between Angola and Nigeria westwardly extended to the central equatorial Atlantic resemble those of the equatorial mode previously noted for the boreal summer [*Zebiak*, 1993; *Wagner and da Silva*, 1994]. Relatively weak but significant positive SST anomalies are also noted in a small area in the central South Atlantic between 30°S and 45°S. The associated SLP anomaly pattern shows quite well defined centers over Australia/western Pacific (negative) and over the Bering Sea/Aleutian region (positive), and considerably weak anomalies elsewhere in the globe (Figure 3e). In the eastern tropical Pacific, although weak, there are hints of positive SLP anomalies which are consistent with the negative SST anomalies in this sector. On the other hand, the absence of above normal SLP anomalies in the region with anomalously colder than normal surface waters in the eastern equatorial Atlantic indicates a relatively weak ocean-atmosphere coupling in this region.

[25] This weak ocean-atmosphere coupling might result from the competing effects of the large and regional scale circulation anomalies. While the LN induces the establishment of above normal SLP anomalies in the tropical North Atlantic [*Covey and Hastenrath*, 1978; *Saravanan and Chang*, 2000], the negative SST anomalies in the eastern equatorial Atlantic tend to create below normal SLP anomalies to the north. These competing effects yield reduced SLP anomalies in the tropical Atlantic. However, the regional circulation overwhelming the LN teleconnec-

tion yield negative SLP anomalies over northeastern Venezuela, Guyana, Surinam, French Guiana and surrounding tropical North Atlantic area (Figure 3e). The below normal SLP anomalies in the tropical North Atlantic and the presence of colder than normal surface waters along the central equatorial Atlantic are indicative of a northward displaced ITCZ. This explains the observed rainfall anomaly pattern with opposite sign values over NEB (negative) and over northeastern Venezuela, Guyana, Surinam and French Guiana (positive) (Figure 2b). Moreover, the colder than normal surface waters in the equatorial and tropical South Atlantic might inhibit the actions of synoptic phenomena such as slow moving cold fronts and subtropical upper tropospheric cyclonic vortices in producing rainfall. These systems play an important role in modulating the rainfall in eastern and northeastern Brazil during the austral spring, summer and fall seasons [*Kousky*, 1979; *Kousky and Gan*, 1981].

[26] The mean SST anomaly pattern for the DRY-NE case shows an ENSO neutral condition as indicated by the small areas of the eastern Pacific with significant positive values (Figure 3c). In the tropical Atlantic, positive anomalies are centered in the southwestern sector between 30°S and 45°S, and to the north a positive meridional SST anomaly gradient pattern is established. This gradient pattern shows warmer than normal surface waters in the tropical North Atlantic near the coast of Africa and colder than normal surface waters along the coast of Angola and off the east coast of the NEB. The positive meridional SST anomaly gradient and the dry conditions in the NEB are consistent with previous findings [*Hastenrath and Heller*, 1977; *Moura and Shukla*, 1981; *Nobre and Shukla*, 1996; *Souza et al.*, 2000]. The associated SLP anomaly pattern shows small magnitude anomalies in most of the study domain (Figure 3f). Although this is also true for the Atlantic, the SLP anomalies in this sector are consistent with the positive meridional SST gradient as well as with the observed dry conditions in the NEB (Figures 3c, 3f, and 2c). Indeed, small magnitude negative SLP anomalies are found in the eastern tropical North Atlantic and over northern Africa, and the positive ones in the tropical South Atlantic, over NEB and over eastern Africa. These results indicate a relatively weak ocean-atmosphere coupling in the tropical Atlantic. This weak ocean-atmosphere coupling might be due to the absence of the ENSO teleconnections.

[27] The wet composites of SST and SLP anomalies are displayed in Figure 4. In general, the SST and SLP anomaly composites for the WET-LN, WET-EN and WET-NE cases show approximately reversed patterns of the DRY-EN, DRY-LN and DRY-NE cases, respectively. The SST anomaly composite for the WET-LN case shows LN-related pattern with the colder than normal surface waters in the central and eastern equatorial Pacific and the warmer than normal surface waters to the north and to the south. In the tropical North Atlantic, the negative pattern resembles that of the interannual mode externally forced by the ENSO described in previous work [*Enfield and Mayer*, 1997; *Saravanan and Chang*, 2000] (Figure 4a). The negative SST anomalies in the tropical North Atlantic and the weak positive SST anomalies in the band between equator and 15°S form a negative meridional SST anomaly gradient. It is interesting to note an area with warmer than normal surface waters in the southwest Atlantic. The DRY-EN case does not show a correspondent area with opposite sign anomalies. The SLP anomaly composite for the WET-LN case features below normal SLP anomalies over Australasia, western tropical Pacific, Iceland and in the eastern tropical South Atlantic and above normal SLP anomalies in the tropical North Atlantic (Figure 4d). Weak positive SLP anomalies are noted in southeast Pacific. The consistent meridional anomaly SLP (positive) and SST (negative) gradients in the tropical Atlantic and the observed excessive rainfall over NEB are coherent with previous findings [*Hastenrath and Heller*, 1977; *Moura and Shukla*, 1981].

[28] The SST anomaly composite for the WET-EN case features a EN pattern with significant positive values extending from the central equatorial Pacific toward Central America, and relatively weak anomalies elsewhere in the Pacific basin, except for the significant negative values centered in the southeastern Pacific at approximately (35°S, 110°W) (Figure 4b). This composite also shows warmer than normal surface waters in the Caribbean Sea, in the equatorial Atlantic and in the central tropical South Atlantic, and colder than normal surface waters in the southwestern Atlantic centered at approximately (35°S, 30°W). The positive SST anomalies along the equatorial Atlantic resemble those of the equatorial mode described by *Wagner and da Silva* [1994]. The associated SLP anomaly pattern shows significant positive values over the western tropical Pacific, and small anomalies elsewhere (Figure 4e). Likewise the DRY-LN case, the WET-EN case shows a relatively weak ocean-atmosphere coupling in particular in the equatorial and tropical South Atlantic. Similar to the previous analysis, this might result from the competing effects of the EN and the SST variability in the equatorial and tropical South Atlantic. While, the EN remotely induces below normal SLP anomalies in the tropical North Atlantic [*Covey and Hastenrath*, 1978; *Saravanan and Chang*, 2000], the positive SST anomalies in the equatorial and tropical South Atlantic induce above normal SLP anomalies in the same region. These effects yield reduced SLP anomalies in the tropical Atlantic. However, the regionally induced SLP anomalies are more dominant in such a way that weak positive SLP anomalies are noted over northeastern Venezuela, Guyana, Surinam, French Guiana and in the adjacent Atlantic area. The positive SST anomalies along the equatorial Atlantic and the positive SLP anomalies to the north favor the southward location of the ITCZ [*Hastenrath and Heller*, 1977]. This location of the ITCZ is consistent with the enhanced rainfall over NEB and the reduced rainfall over northeastern Venezuela, Guyana, Surinam and French Guiana (Figure 2e). Moreover, warmer than normal surface waters in the equatorial and tropical South Atlantic might locally favor the actions of synoptic scale phenomena (cold fronts and upper tropospheric cyclonic vortices) in producing rainfall over the NEB.

[29] The SST anomaly composite for the WET-NE case presents significant negative values in the eastern equatorial Pacific and in the southwestern Atlantic between 30°S and 40°S, and positive ones along the equatorial Atlantic and in small areas of the tropical South Atlantic, and insignificant anomalies elsewhere (Figure 4c). The associated SLP anomaly pattern shows considerably weak anomalies in most of the study domain (Figure 4f). Although the SLP

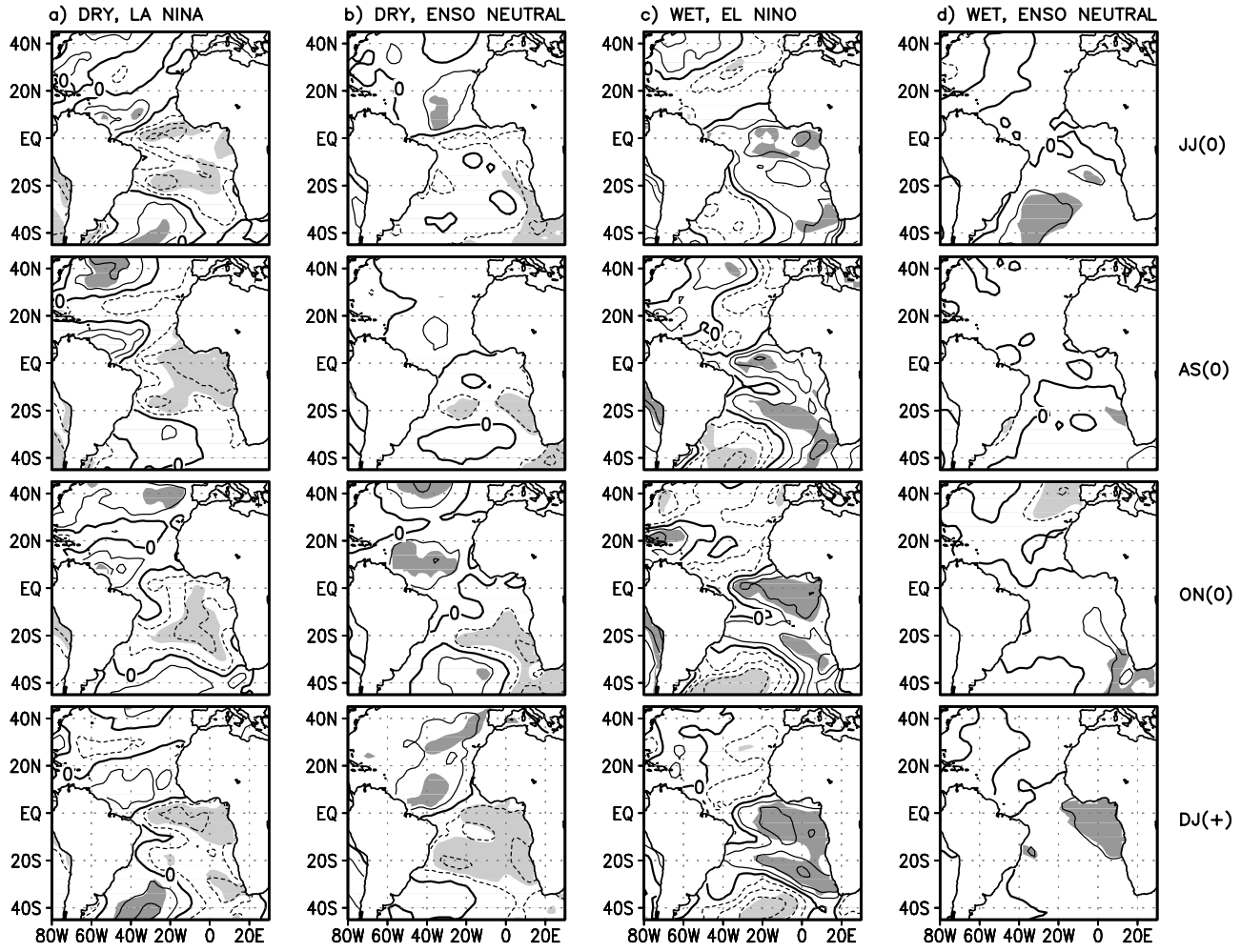

Figure 5. Bimonthly mean normalized SST anomalies for the 2 months indicated at the right for (a) DRY-La Niña, (b) DRY-ENSO neutral (c) WET-El Niño, and (d) WET-ENSO neutral. Display is the same as that in Figure 3.

anomalies are considerably weak, warmer than normal surface waters along the equatorial Atlantic favor the southward location of the ITCZ. Moreover, the warmer than normal surface waters might favor the actions of the synoptic scale systems (cold fronts and upper tropospheric cyclonic vortices) in producing rainfall. This explains the positive rainfall anomalies observed over the northern sector of NEB. These results reinforce previous findings that in the absence of the ENSO teleconnections, the strongest correlations are found between the NEB rainfall and the SST variability in the tropical South Atlantic [*Saravanan and Chang*, 2000].

3.4. SST Bimonthly Composites

[30] *Gianni et al.* [2004] provided modeling and observational evidences that the ENSO and tropical Atlantic variability relations during the NEB rainy season might be affected by the tropical Atlantic SST preconditions existing up to 6 months before. They focused on the SST dipole mode in the tropical Atlantic. Following a similar approach, differences between the canonical cases (DRY-EN and WET-LN) and the other cases are investigated here using the SST anomalous preconditions in the tropical Atlantic. So, bimonthly composites of the SST anomalies in this oceanic sector for June$^{(0)}$–July$^{(0)}$, August$^{(0)}$–September$^{(0)}$, October$^{(0)}$–November$^{(0)}$, and December$^{(0)}$–January$^{(+)}$ periods (indicated as JJ$^{(0)}$, AS$^{(0)}$, ON$^{(0)}$, and DJ$^{(+)}$) are obtained for all cases. The symbols '$^{(0)}$' and '$^{(+)}$' indicate the year before the rainy season and of the rainy season, respectively.

[31] The Atlantic SST anomaly composites for the DRY-LN case during DJ$^{(+)}$ and FMA show a quite similar pattern (Figures 5a and 3b). However, hints of this pattern can be followed back up to JJ$^{(0)}$. The sequential bimonthly composites evidences a persistent and spatially coherent SST anomaly pattern with significant negative values in a large area which includes the equatorial and tropical South Atlantic and relatively weak opposite sign values to the north (Figure 5a). This persistent positive meridional SST anomaly gradient pattern conflicts with the LN-related pattern in the tropical Atlantic. The expected pattern for a LN is a negative meridional SST anomaly gradient, mainly due to the cooling of the surface waters in the tropical North Atlantic [*Enfield and Mayer*, 1997; *Saravanan and Chang*, 2000].

[32] The Atlantic SST anomaly composites for the WET-EN case during DJ$^{(+)}$ and FMA show a similar pattern with

dominance of positive SST anomalies in the equatorial and tropical South Atlantic (Figures 5c and 4b). As above, hints of this pattern indicated by significant positive SST anomalies in the equatorial and southeastern Atlantic and by weak negative ones in the tropical North Atlantic are evident in $JJ^{(0)}$. In the subsequent bimonthly composites, the significant positive anomalies persist and intensify. This negative meridional SST anomaly gradient pattern contrasts with the expected warming of the surface waters in the tropical North Atlantic associated with an EN [*Enfield and Mayer*, 1997; *Saravanan and Chang*, 2000].

[33] The persistent character of the tropical Atlantic SST pattern with significant negative anomalies in the tropical South Atlantic and positive anomalies to the north is also noted for the DRY-NE case (Figure 5b). In this case, the dipolar structure is more pronounced only for the two bimonthly composites before the NEB rainy season.

[34] The bimonthly composites of the SST anomalies for the WET-NE case show relatively small values compared with those of the other three cases (Figure 5d). However, the WET-NE case also shows hints of positive anomalies in the tropical South Atlantic and of negative anomalies in the tropical North Atlantic during the periods from $JJ^{(0)}$ to $DJ^{(+)}$. Nevertheless, the areas with the largest anomalies are not coincident among the bimonthly composites.

[35] The canonical DRY-EN and WET-LN cases show different evolutions compared to those of the DRY-LN and WET-EN. The sequential bimonthly SST anomaly composites for WET-LN show a relatively persistent pattern with positive anomalies in the equatorial and tropical South Atlantic and negative anomalies in the Caribbean Sea (Figure 6b). This pattern is consistent with the LN-induced SST in the tropical Atlantic. As the ENSO teleconnection is strong in the tropical North Atlantic during austral fall [*Enfield and Mayer*, 1997], the LN reinforces the preexisting negative SST anomalies in the tropical North Atlantic (Figure 4a). Consistent with this result, *Gianni et al.* [2004] showed that the tropical Atlantic variability can precondition the development of the ENSO teleconnection, reinforcing (as the case analyzed here) or weakening it.

[36] On the other hand, the DRY-EN bimonthly composites show a more horizontal structure without a persistent and spatially coherent SST anomaly pattern. *Gianni et al.* [2004] suggested that in the absence of a well established precondition in the tropical Atlantic, the ENSO teleconnection induces SST anomalies in the tropical North Atlantic of the same sign as those in the eastern equatorial Pacific. This is the case of the DRY-EN composite presented here.

4. Conclusions

[37] Climate extremes (dry and wet) over NEB stratified according to the ENSO (EN, LN and NE) phases of the preceding year are used to reexamine the precipitation anomaly patterns over northern and northeastern South America and the associated SST and SLP variability modes. Analyses are done using the composite technique for NEB rainy seasons (FMA) of the 1913–1998 period.

[38] Classification of the NEB rainy seasons in dry, normal and wet categories stratified by the ENSO phases

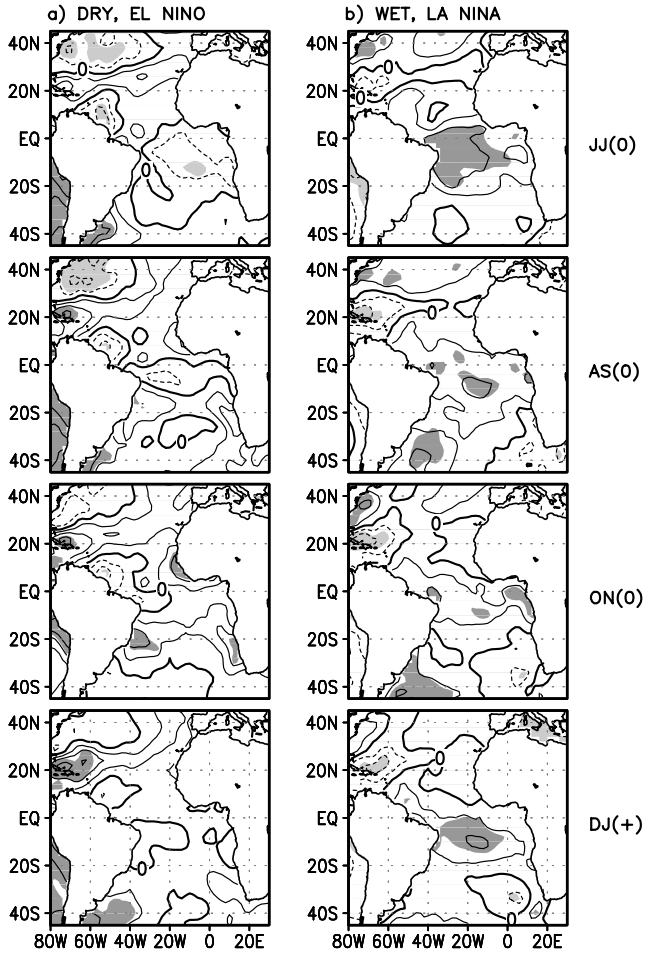

Figure 6. Bimonthly mean normalized SST anomalies for the 2 months indicated at the right for (a) DRY- El Niño and (b) WET- La Niña. Display is the same as that in Figure 3.

provides indications that the relationship between the ENSO and the NEB rainfall variability is quite weak. Of the total 86 rainy seasons, 19 with climate extremes comply with the known ENSO relationship and 12 with normal climate conditions are preceded by ENSO neutral conditions. These 31 rainy seasons represent 36% of the total 86 rainy seasons. Thus 36% of the time an ENSO-based climate forecast for the NEB would be right. This percentage is lower than that (50%) found by *Kane* [1997] for the droughts forecast based on the occurrence of EN. Therefore ENSO-based forecast for the NEB climate might even be worse than that pointed out by *Kane* [1997].

[39] The SST and SLP anomaly composites for the canonical DRY-EN and WET-LN cases feature approximately reversed sign patterns with ENSO coherent signature in the tropical Pacific and in the tropical North Atlantic. These patterns are highly consistent with previous findings on the ENSO relationship with the tropical Atlantic variability [*Enfield and Mayer*, 1997; *Saravanan and Chang*, 2000]. For these cases, the ENSO teleconnections in the tropical Atlantic result in a meridional SST anomaly gradient with the largest amplitude of anomalies in the tropical North Atlantic, which show the same sign as those in the eastern equatorial Pacific. The associated precipitation

anomaly composites reflect, in part, the linear component of the NEB climate response to the combined effect of the eastern equatorial Pacific and tropical Atlantic SST variability and show regional rainfall anomaly patterns highly consistent with previous findings [*Ropelewski and Halpert*, 1987, 1989; *Rao and Hada*, 1990; *Uvo et al.*, 1998; *Souza et al.*, 2000].

[40] Conversely, the DRY-LN, DRY-NE, WET-EN and WET-NE cases do not show strong links with the ENSO. Rather, the tropical Atlantic variability modes seem to play a more crucial role in these cases. In particular for the DRY-LN, a positive meridional SST anomaly pattern is established in the tropical Atlantic due to the strong negative SST anomalies in the equatorial and tropical South Atlantic. This pattern overwhelms the expected LN-induced negative SST anomalies in the tropical North Atlantic. The associated SLP anomalies show a consistent but weak negative meridional SLP pattern in the tropical Atlantic. The WET-EN case shows similar SST and SLP patterns but with opposite signs. The weak ocean-atmosphere coupling in the tropical Atlantic for the DRY-LN and WET-EN cases can be explained by the competing effects of the ENSO teleconnections and regional SST variability. On the other hand, the DRY-NE and WET-NE cases also show weak ocean-atmosphere coupling in the tropical Atlantic. This is particularly conspicuous for the DRY-NE case. These results suggest that the ENSO teleconnections affect the thermodynamic feedback to reinforce the ocean-atmosphere coupling (SST, wind and evaporation) as well as the SST anomalies damping through the meridional ocean heat transport proposed by *Chang et al.* [1997]. So, the ocean-atmosphere coupling in the tropical Atlantic is reinforced under ENSO-coherent SST anomalies in the tropical Atlantic; this coupling is weakened under ENSO neutral conditions or when the SST anomalies in the tropical Atlantic show opposite signs than those expected for the ENSO teleconnections.

[41] The precipitation patterns for the DRY-LN, DRY-NE, WET-EN and WET-NE cases illustrate the opposite sign precipitation anomalies over NEB and over the region from northeastern Venezuela to French Guiana pointed out in previous studies [*Hastenrath and Heller*, 1977; *Hastenrath*, 1978]. These patterns might be explained by the associated SST patterns in the equatorial and tropical South Atlantic, which might affect the meridional displacements of the ITCZ and the actions of the synoptic scale systems (slow moving cold fronts and upper tropospheric cyclonic vortices) on the NEB climate. These synoptic systems play an important role in modulating the rainfall in eastern and northeastern Brazil during the austral spring, summer and fall seasons [*Kousky*, 1979; *Kousky and Gan*, 1981].

[42] An interesting aspect revealed in the present analysis is that hints of the FMA SST anomaly patterns in the tropical Atlantic for the DRY-LN, DRY-NE and WET-EN composites can be followed back to $JJ^{(0)}$. Support to this result is given by *Gianni et al.* [2004] who proposed that the tropical Atlantic can precondition the ENSO teleconnection in this sector. These hints are particularly strong in the tropical South Atlantic. This result indicates that the SST variations in the tropical Atlantic, in particular in its southern sector during months prior to the rainy season should be carefully monitored in the diagnostic activities.

[43] **Acknowledgments.** The authors are grateful to the three anonymous reviewers for their useful comments and suggestions. The authors were partially supported by the Conselho Nacional de Desenvolvimento Cientıacute;fico and Tecnológico of Brazil. Thanks are owed to the UK Meteorological Office (UKMO) for the provision of the sea level pressure data used in this paper. Thanks are also owed to Mike Hulme for the provision of "gu23wld0098.dat" (version 1.0) constructed at the Climatic Research Unit, University of East Anglia, Norwich, UK.

References

Aceituno, P. (1988), On the functioning of the Southern Oscillation in the South American sector. Part 1: Surface climate, *Mon. Weather Rev.*, *116*, 505–524.

Andreoli, R. V., and M. T. Kayano (2003), Evolution of the equatorial and dipole modes of the sea surface temperature in the tropical Atlantic at decadal scale, *Meteorol. Atmos. Phys.*, *83*, 277–285.

Barros, V. R., and G. E. Silvestri (2002), The relation between sea surface temperature at the subtropical south-central Pacific and precipitation in southeastern South America, *J. Clim.*, *15*, 251–267.

Caviedes, C. N. (1973), Secas and El Niño: Two simultaneous climatical hazards in South America, *Proc. Assoc. Am. Geograph.*, *5*, 44–49.

Chang, P., L. Ji, and H. Li (1997), A decadal climate variation in the tropical Atlantic Ocean from thermodynamic air-sea interactions, *Nature*, *385*, 516–518.

Covey, D., and S. Hastenrath (1978), The Pacific El Niño phenomenon and the Atlantic circulation, *Mon. Weather Rev.*, *106*, 1280–1287.

Enfield, D. B., and D. A. Mayer (1997), Tropical Atlantic sea surface temperature variability and its relation to El Niño–Southern Oscillation, *J. Geophys. Res.*, *102*, 929–945.

Enfield, D. B., A. Mestas-Nuñez, D. A. Mayer, and L. Cid-Serrano (1999), How ubiquitous is the dipole relationship in tropical Atlantic sea surface temperatures, *J. Geophys. Res.*, *104*, 7841–7848.

Giannini, A., R. Saravanan, and P. Chang (2004), The preconditioning role of tropical Atlantic variability in the development of the ENSO teleconnection: Implications for the prediction of Nordeste rainfall, *Clim. Dyn.*, *22*, 839–855, doi:10.1007/s00382-004-0420-2.

Hastenrath, S. (1978), On modes of tropical circulation and climate anomalies, *J. Atmos. Sci.*, *35*, 2222–2231.

Hastenrath, S. (1990), Prediction of northeast Brazil rainfall anomalies, *J. Clim.*, *3*, 893–904.

Hastenrath, S., and L. Greischar (1993), Circulation mechanisms related to northeast Brazil rainfall anomalies, *J. Geophys. Res.*, *98*, 5093–5102.

Hastenrath, S., and L. Heller (1977), Dynamics of climatic hazards in northeast Brazil, *Q. J. R. Meteorol. Soc.*, *103*, 77–92.

Horel, J. D., and J. M. Wallace (1981), Planetary-scale atmospheric phenomena associated with the Southern Oscillation, *Mon. Weather Rev.*, *10*, 813–829.

Hulme, M. A. (1992), 1951–80 global land precipitation climatology for the evaluation of general circulation models, *Clim. Dyn.*, *7*, 57–72.

Hulme, M. A. (1994), Validation of large-scale precipitation fields in general circulation models, in *Global Precipitations and Climate Change*, *NATO ASI Ser., Ser. I*, vol. 26, edited by M. Desbois and F. Desalmand, pp. 387–406, Springer, New York.

Hulme, M. A., T. J. Osborn, and T. C. Johns (1998), Precipitation sensitivity to global warming: Comparison of observations with HadCM2 simulations, *Geophys. Res. Lett.*, *25*, 3379–3382.

Kane, R. P. (1992), El Niño and La Niña events and rainfall in NE and south Brazil, *Rev. Bras. Geofiacute;s.*, *10*, 49–59.

Kane, R. P. (1997), Prediction of droughts in north-east Brazil: Role of ENSO and use of periodicities, *Int. J. Climatol.*, *17*, 655–665.

Kayano, M. T., V. B. Rao, and A. D. Moura (1988), Tropical circulations and the associated rainfall anomalies during two contrasting years, *J. Climatol.*, *8*, 477–488.

Kiladis, G., and H. F. Diaz (1989), Global climatic anomalies associated with extremes in the Southern Oscillation, *J. Clim.*, *2*, 1069–1090.

Kousky, V. E. (1979), Frontal influences on northeast Brazil, *Mon. Weather Rev.*, *107*, 1140–1153.

Kousky, V. E., and M. A. Gan (1981), Upper tropospheric cyclonic vortices in the tropical South Atlantic, *Tellus*, *33*, 538–551.

Kousky, V. E., and C. F. Ropelewski (1989), Extremes in the Southern Oscillation and their relationship to precipitation anomalies with emphasis on the South American region, *Rev. Bras. Meteorol.*, *4*, 351–363.

Kousky, V. E., M. T. Kayano, and I. F. A. Cavalcanti (1984), A review of the Southern Oscillation: Oceanic-atmospheric circulation changes and related rainfall anomalies, *Tellus, Ser. A*, *36*, 490–504.

Markham, C. G., and D. R. Mclain (1977), Sea surface temperature related to rain in Ceará, *Nnortheastern Brazil, Nature*, *265*, 320–323.

Mehta, V. M. (1998), Variability of the tropical ocean surface temperatures at decadal-multidecadal timescales. Part I: The Atlantic Ocean, *J. Clim.*, *11*, 2351–2375.

Mehta, V. M., and T. Delworth (1995), Decadal variability of the tropical Atlantic Ocean surface temperature in shipboard measurements and in a global ocean-atmosphere model, *J. Clim.*, *8*, 172–190.

Moura, A. D., and J. Shukla (1981), On the dynamics of droughts in northeast Brazil: Observations, theory and numerical experiments with a general circulation model, *J. Atmos. Sci.*, *38*, 2653–2675.

Nobre, P., and J. Shukla (1996), Variations of sea surface temperature, wind stress and rainfall over the tropical Atlantic and South America, *J. Clim.*, *9*, 2464–2479.

Panofsky, H. A., and G. W. Brier (1968), *Some Applications of Statistics to Meteorology*, 224 pp., Pa. State Univ., University Park.

Pezzi, L. P., and I. F. A. Cavalcanti (2001), The relative importance of ENSO and tropical Atlantic SST anomalies for seasonal precipitation over South America: A numerical study, *Clim. Dyn.*, *17*, 205–212.

Pinkayan, S. (1966), Conditional probabilities of occurrence of wet and dry years over a large continental area, *Hydrol. Pap. 12*, Colo. State Univ., Fort Collins.

Rajagopalan, B., Y. Kushnir, and Y. M. Tourre (1998), Observed decadal midlatitude and tropical Atlantic climate variability, *Geophys. Res. Lett.*, *25*, 3967–3970.

Rao, V. B., and K. Hada (1990), Characteristics of rainfall over Brazil: Annual and variations and connections with the Southern Oscillation, *Theor. Appl. Climatol.*, *42*, 81–91.

Rasmusson, E. M., and T. H. Carpenter (1982), Variations in tropical sea surface temperature and surface wind fields associated with the Southern Oscillation/El Niño, *Mon. Weather Rev.*, *110*, 354–384.

Ropelewski, C. F., and M. S. Halpert (1987), Global and regional scale precipitation patterns associated with the El Niño/Southern Oscillation, *Mon. Weather Rev.*, *115*, 1606–1626.

Ropelewski, C. F., and M. S. Halpert (1989), Precipitation patterns associated with the high index phase of the Southern Oscillation, *J. Clim.*, *2*, 268–284.

Saravanan, R., and P. Chang (2000), Interaction between tropical Atlantic variability and El Niño–Southern Oscillation, *J. Clim.*, *13*, 2177–2194.

Servain, J. (1991), Simple climatic indices for the tropical Atlantic Ocean and some applications, *J. Geophys. Res.*, *96*, 15,137–15,146.

Smith, T. M., and R. W. Reynolds (2003), Extended reconstruction of global sea surface temperatures based on COADS data (1854–1997), *J. Clim.*, *16*, 1495–1510.

Souza, E. B., M. T. Kayano, J. Tota, L. Pezzi, G. Fisch, and C. Nobre (2000), On the influences of the El Niño, La Niña and Atlantic dipole pattern on the Amazonian rainfall during 1960–1998, *Acta Amaz.*, *30*, 305–318.

Tourre, Y. M., B. Rajagopalan, and Y. Kushnir (1999), Dominant patterns of climate variability in the Atlantic Ocean during the last 136 years, *J. Clim.*, *12*, 2285–2299.

Trenberth, K. E. (1997), The definition of El Niño, *Bull. Am. Meteorol. Soc.*, *78*, 2771–2777.

Uvo, C. R. B., C. A. Repelli, S. E. Zebiak, and Y. Kushnin (1998), The relationships between tropical Pacific and Atlantic SST and northeast Brazil monthly precipitation, *J. Clim.*, *11*, 551–562.

Wagner, R. G., and A. M. da Silva (1994), Surface conditions associated with anomalous rainfall in the Guinea coastal region, *Int. J. Climatol.*, *14*, 179–199.

Walker, G. T. (1927), World Weather III, *Mem. R. Meteorol. Soc. London*, *2*, 97–107.

Weare, B. C. (1977), Empirical orthogonal analysis of Atlantic Ocean surface temperatures, *Q. J. R. Meteorol. Soc.*, *103*, 467–478.

Zebiak, S. E. (1993), Air-sea interaction in the equatorial Atlantic region, *J. Clim.*, *6*, 1567–1586.

R. V. Andreoli and M. T. Kayano, Instituto Nacional de Pesquisas Espaciais, Centro de Previsão de Tempo e Estudos Climáticos, Avenida dos Astronautas, 1758, 12227-010 São José dos Campos, SP, Brazil. (mary@cptec.inpe.br)